JOC The Journal of Organic Chemistry

Article

pubs.acs.org/joc

Synthesis and Structure of 3,3-Dimethylindoline Squaraine Rotaxanes

Tia S. Jarvis, Carleton G. Collins, Janel M. Dempsey, Allen G. Oliver, and Bradley D. Smith*

Department of Chemistry and Biochemistry, University of Notre Dame, 236 Nieuwland Science Hall, Notre Dame, Indiana 46556, United States

Supporting Information

ABSTRACT: Squaraine rotaxanes are mechanically interlocked molecules comprised of a dumbbell shaped squaraine dye inside a tetralactam macrocycle. Previous squaraine rotaxanes have employed planar squaraine dyes with 4-aminophenyl, 2-aminothiophene, or *N*-amino units appended to the central C_4O_2 core. Here we describe two rotaxanes that encapsulate a 3,3-dimethylindoline squaraine inside a tetralactam with anthracene sidewalls. The rotaxanes were prepared by a templated clipping reaction and an X-ray crystal structure shows that the squaraine *gem*-dimethyl groups force a relatively wide separation between the macrocycle anthracene sidewalls. The decreased interaction between the encapsulated squaraine and the anthracene sidewalls leads to a smaller red shift of the squaraine absorption and emission bands. Solution-state studies show that the *gem*-dimethyl groups in 3,3-dimethylindoline squaraine dyes are large enough to prevent macrocycle threading or rotaxane unthreading. One of the new rotaxanes emits an orange light (560−650 nm), and there is a 10-fold enhancement in the squaraine fluorescence quantum yield upon encapsulation as a rotaxane. This orange-emitting dye completes the palette of known squaraine rotaxane fluorophores whose emission profiles span the color range from green to near-infrared.

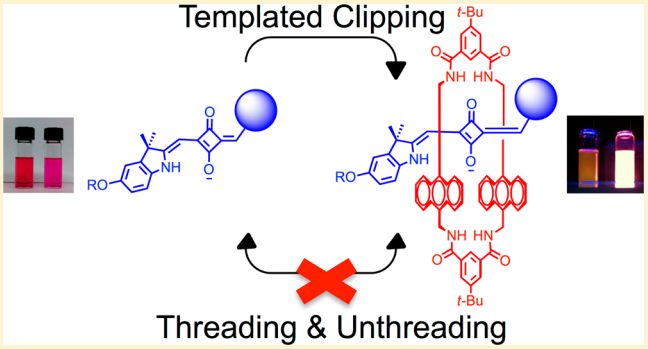

INTRODUCTION

A current topic in supramolecular research is encapsulation of fluorophores inside container molecules to form host−guest complexes with improved photophysical performance.[1−3] These customized, functional supramolecular architectures have potential applications in a wide range of chemical fields including analytical, biological, pharmaceutical, and materials science.[1,2] We have contributed to this endeavor by inventing squaraine rotaxanes, mechanically interlocked molecules comprised of a dumbbell shaped squaraine dye inside a tetralactam macrocycle.[3,4] The encapsulation process has been shown to greatly improve squaraine chemical stability and also alter fluorescence properties. Squaraine rotaxanes with appended targeting groups act as effective molecular probes for fluorescence microscopy and *in vivo* imaging of living subjects.[5] Furthermore, systematic modification of the encapsulated squaraine and the surrounding macrocycle has led to squaraine rotaxanes with sensing capabilities[6] and thermally activated chemiluminescence.[7] An important spectral feature is the narrow absorption and emission bands, which favor multicolor imaging protocols using a mixture of dyes with different wavelengths. There is also the possibility of multiplex imaging using squaraine rotaxanes with macrocycles containing anthracene sidewalls. In this case, UV excitation of the anthracene units is followed by internal fluorescence energy transfer to the encapsulated squaraine which subsequently emits the light at its characteristic longer wavelength.

All of our previous squaraine rotaxanes have employed planar squaraine dyes with 4-aminophenyl, 2-aminothiophene, or *N*-amino units appended to the central C_4O_2 core. This work has produced mechanically interlocked molecules with near-infrared, deep-red, and green absorption/emission wavelengths.[8] An obvious gap in the squaraine rotaxane emission palette is an orange-emitting fluorophore. Several different squaraine structures are known to emit orange light,[9] but the most synthetically accessible seemed to be 3,3-dimethylindoline derivatives.[10] When contemplating rotaxanes that encapsulate a 3,3-dimethylindoline squaraine dye, the obvious first question is whether the steric size of the *gem*-dimethyl groups on the squaraine structure prevents rotaxane formation.[11] If dye encapsulation can be achieved, the next question is whether the *gem*-dimethyl groups are large enough to prevent rotaxane threading/unthreading.[12] Would encapsulation of a 3,3-dimethylindoline squaraine dye as a rotaxane alter its photophysical properties? Here we address these questions by describing the syntheses, structures, and spectral properties of two novel 3,3-dimethylindoline squaraine rotaxanes, the orange

Received: March 20, 2017
Published: May 18, 2017

DOI: 10.1021/acs.joc.7b00655
J. Org. Chem. 2017, 82, 5819−5825

emitting **M1** ⊃ **1** and the more sterically crowded **M1** ⊃ **2** (Scheme 1).

Scheme 1. Chemical Structures and Atom Labels

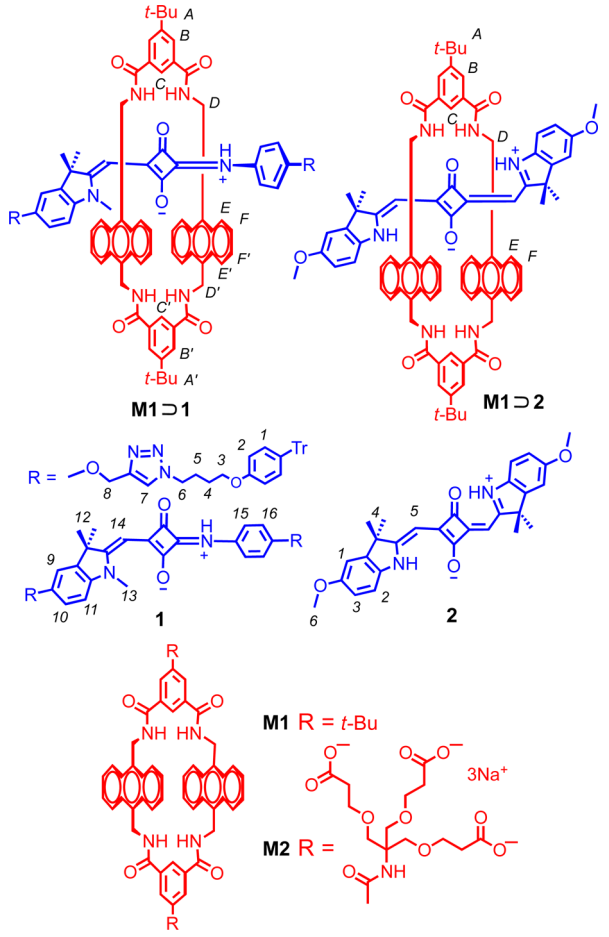

RESULTS AND DISCUSSION

Synthesis and Structure of Orange Emitting M1 ⊃ 1. As a prudent first synthetic goal, we chose to prepare **M1** ⊃ **1**, a rotaxane that encapsulates the sterically less congested asymmetric squaraine, **1**, with only one adjacent 3,3-dimethylindoline unit and a large phenoxytrityl stopper group linked to each end of the dyes. The synthetic sequence to produce **M1** ⊃ **1** is detailed in Scheme 2. The known aniline **3** was converted to hydrazine **4** and then reacted with 3-methyl-2-butanone under Fischer indole synthesis conditions to give indole **5**. Methylation of **5** produced the indolium salt which was not purified but condensed with diethyl squarate to give the semisquaraine **6**. Subsequent reaction of **6** with **3** gave the asymmetric bis-alkyne squaraine **7** in good yield. Mixing **7** with macrocycle **M1** in $CHCl_3$ produced the reversible pseudorotaxane complex **M1** ⊃ **7** which was covalently capped by conducting a copper catalyzed azide alkyne cycloaddition with 2 molar equiv of azide **8** to give the permanently interlocked rotaxane **M1** ⊃ **1** in 71% yield. A separate synthetic procedure reacted **7** with 2 molar equiv of **8** to give the free dye **1**.

The absorption/emission properties of **1** and **M1** ⊃ **1** are compared in Table 1.[13] The emission band for **M1** ⊃ **1** is between 560 and 650 nm, making it an orange emitting fluorophore. The quantum yield of **1** is increased by an order of

Scheme 2. Synthesis of M1 ⊃ 1

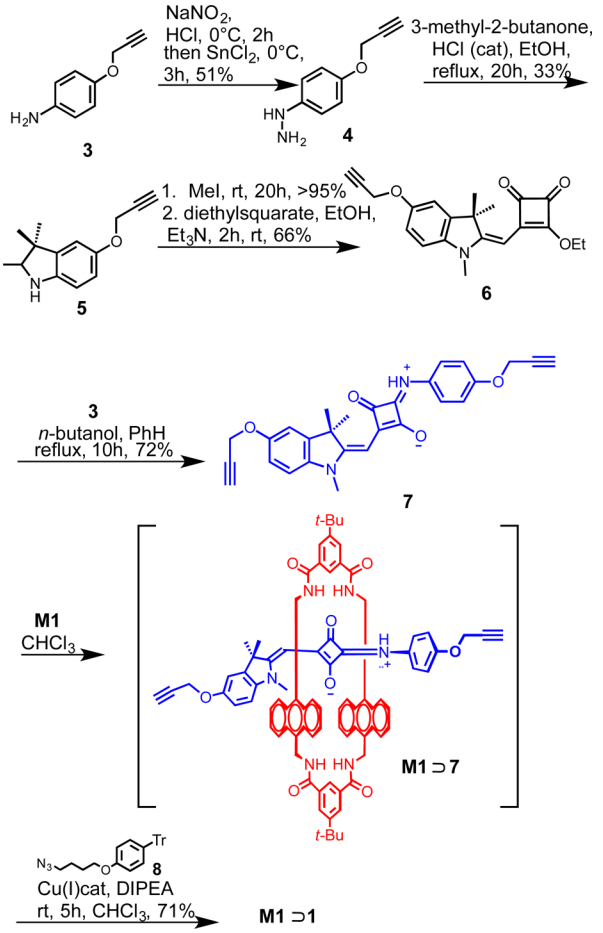

Table 1. Photophysical Data for M1 ⊃ 1 and 1

compd	λ_{abs} (nm)	λ_{em} (nm)	log ε (M^{-1} cm^{-1})	Φ_f[a]
1	539	561	4.83	0.04
M1 ⊃ **1**	554	575	4.60	0.44
2	677	698	5.11	0.14
M1 ⊃ **2**	688	708	4.75	0.09

[a]Quantum yield measurements (±5%) were determined in $CHCl_3$ using 4,4-[bis(*N*,*N*- dimethylamino)phenyl]squaraine dye as a reference (Φ_f = 0.70 in $CHCl_3$).

magnitude when it is encapsulated as **M1** ⊃ **1**, resulting in a fluorophore that is 6.3 times brighter than the unencapsulated squaraine. The dramatic enhancement in fluorescence brightness is illustrated by the photographic images in Figure 1. An increase in fluorescence quantum yield has been observed previously for other squaraine rotaxanes and is attributed to reduced vibrational and rotational motion of the encapsulated squaraine dye, making nonradiative excited state relaxation pathways less favorable.[8]

The ^{1}H NMR spectrum for rotaxane **M1** ⊃ **1** was quite broad at 20 °C, and the signals sharpened upon cooling (Figure S16). The spectral pattern indicated a lack of vertical or horizontal symmetry in the rotaxane structure and a comparison of the chemical shifts for **M1** ⊃ **1** with the chemical shifts for free dye **1** (Figure S14a; see Scheme 1 for atom labels) revealed the following structural information. (a) Separate signals for the two macrocycle protons C in **M1** ⊃ **1** implied slow pirouetting of the surrounding macrocycle around

DOI: 10.1021/acs.joc.7b00655
J. Org. Chem. 2017, 82, 5819−5825

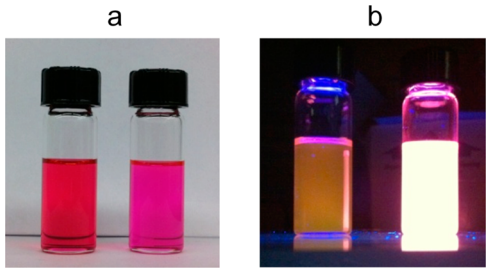

Figure 1. (a) Photograph of solutions containing squaraine **1** (left) and **M1** ⊃ **1** (right) in $CHCl_3$ (20 μM). (b) Same solutions illuminated with long-range UV light.

the encapsulated asymmetric squaraine. (b) Chemical shifts for squaraine aryl protons 15 and 16 in **M1** ⊃ **1** were significantly upfield of the same protons in free **1**, suggesting that they were situated within the surrounding macrocycle. (c) Chemical shifts for the *gem*-dimethyl protons 12 in free **1** and **M1** ⊃ **1** were similar, suggesting that the *gem*-dimethyl groups in **M1** ⊃ **1** were not inside the surrounding macrocycle. (d) Chemical shifts for the triazole protons 7 and 18 in free **1** and **M1** ⊃ **1** were similar, suggesting that the triazole protons in **M1** ⊃ **1** were not inside the macrocycle. Combined, the chemical shift data strongly suggest that the major coconformation of **M1** ⊃ **1** has the surrounding macrocycle located around the less congested side of the encapsulated squaraine and away from the *gem*-dimethyl groups on the other side (Figure 2).

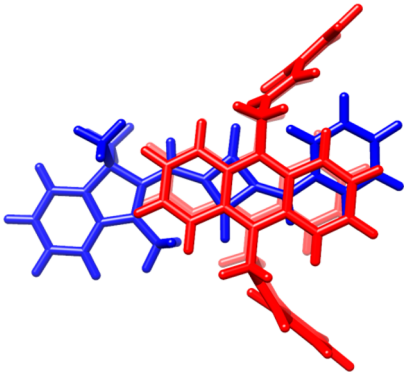

Figure 2. Capped sticks model of the **M1** ⊃ **1** core that illustrates the major coconformation predicted by NMR chemical shift data. The structure was optimized using the semiempirical quantum method at PM7 level.

Synthesis and Structure of Deep-Red Emitting M1 ⊃ 2. After finding that a 3,3-dimethylindoline squaraine dye can be encapsulated by a tetralactam macrocycle, the next step was to determine if the *gem*-dimethyl groups were large enough to block rotaxane threading or unthreading.[12,14−17] We decided to prepare a rotaxane that encapsulated the symmetrical 3,3-dimethylindoline squaraine **2** with proximal *gem*-dimethyl groups on either side of the central C_4O_2 core. This was achieved in two synthetic steps. First, 5-methoxy-2,3,3-trimethylindoline was condensed with squaric acid to give **2** in 41% yield. Then, a templated clipping reaction was conducted that reacted 4-*tert*-butylisophthaloyl dichloride with 9,10-bis(aminomethyl)anthracene in the presence of **2** to obtain **M1** ⊃ **2** in 11% yield (Scheme 3).[18]

The absorption/emission properties of **2** and **M1** ⊃ **2** are compared in Table 1.[13] The emission band for **M1** ⊃ **2** is

Scheme 3. Synthesis of M1 ⊃ 2

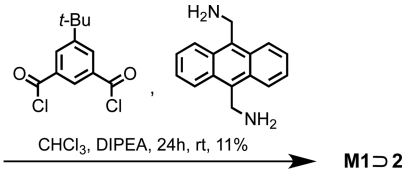

between 688−708 nm, making it a near-infrared emitting fluorophore. The quantum yield of **2** is slightly decreased when it is encapsulated as rotaxane **M1** ⊃ **2**, a striking contrast to the large enhancement in quantum yield reported above.[19]

Single crystals of **M1** ⊃ **2** were grown by slow diffusion. That is, a 3 mM dichloromethane solution of **M1** ⊃ **2** in a loosely capped vial was placed inside a larger vial containing hexanes. A suitable crystal was isolated and subjected to analysis by X-ray diffraction. The molecular structure in Figure 3 shows the

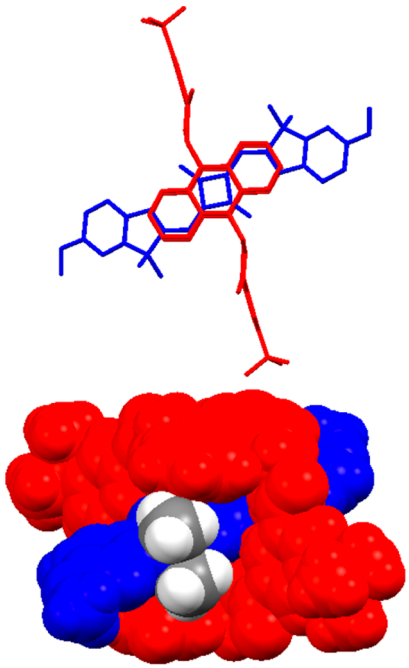

Figure 3. X-ray structure of **M1** ⊃ **2**. (Top) Side view of capped sticks model, (bottom) space-filling projection that emphasizes packing of squaraine gem-dimethyl groups (gray and white) against the periphery of the macrocycle anthracene sidewalls (red).

encapsulated squaraine in trans configuration with both indoline NH residues hydrogen bonded to the adjacent oxygen atom. The surrounding macrocycle adopts a flattened chair conformation with bifurcated hydrogen bonding between the two NH residues and the squaraine oxygens. The centroid-to-centroid distance between the two anthracene sidewalls is 7.6 Å, which is significantly larger than the corresponding distance of 6.9−7.2 Å for previous squaraine rotaxanes with the same surrounding macrocycle but thinner encapsulated squaraines.[20] The wider macrocycle cavity size in **M1** ⊃ **2** helps minimize steric repulsion between the anthracene sidewalls and the squaraine *gem*-dimethyl groups.

Shown in Figure 4 is a comparison of the ^{1}H NMR chemical shifts for **M1** ⊃ **2** and the free components **M1** and **2**. As a free dye, there are two sets of peaks for **2** corresponding to energetically similar cis and trans configurations,[21,22] but only

DOI: 10.1021/acs.joc.7b00655
J. Org. Chem. 2017, 82, 5819−5825

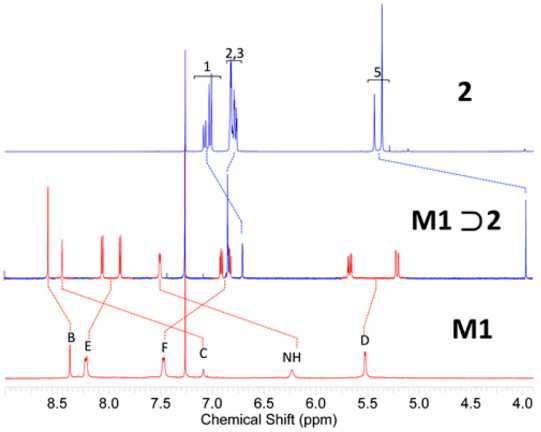

Figure 4. Partial ^{1}H NMR spectra in $CDCl_3$ (600 MHz, at 23 °C) comparing **2**, **M1**, and **M1** ⊃ **2**. See Scheme 1 for atom labels.

the trans configuration is trapped inside the rotaxane. The changes in chemical shift caused by rotaxane formation are very similar to those seen with other squaraine rotaxanes. Most notable is the large downfield change in chemical shift for macrocycle proton C and the upfield change for squaraine proton 5.

The mechanical stability of interlocked **M1** ⊃ **2** was tested by using NMR and UV−vis spectroscopy to monitor samples dissolved in $CHCl_3$ and DMSO. With both solvents, there was no evidence of any rotaxane unthreading after 72 h at 50 °C. We also tested if the *gem*-dimethyl groups in squaraine **2** blocked the reverse process, that is, threading of empty **M1** by squaraine **2**. A binary mixture of free **2** and **M1** was monitored over 72 h time by NMR and UV−vis, with no spectral indication of macrocycle threading. We infer from these results that the *gem*-dimethyl groups in 3,3-dimethylindoline squaraines are sufficiently large to block threading or unthreading of tetralactam **M1** in organic solvents.

Recently, we discovered that the rates of tetralactam threading by squaraine dyes were much faster in water than in chloroform, and one possible corollary of this finding is that the steric barrier to macrocycle threading changes with solvent polarity.[23] We were curious to learn if the *gem*-dimethyl groups could still block macrocycle threading if the process was conducted in water. Therefore, we made the water-soluble 3,3-dimethylindoline squaraine **12** and determined its ability to thread the known tetralactam **M2** in water. As shown in Scheme 4, squaraine **12** was synthesized in two steps from indole **5** and its spectral properties were characterized. A fluorescence experiment compared two separate aqueous samples, a binary mixture of **M2** plus **12** and a mixture of **M2** plus the known 2-aminothiophene squaraine **13**.[24] The mixture of **M2** plus **13** served as a positive control, since we knew that it instantly forms the threaded complex **M2** ⊃ **13**. As expected, mixing **M2** with **13** produced the 15 nm diagnostic red shift in squaraine emission wavelength and also efficient energy transfer from excited **M2** to the encapsulated **13** (top of Figure 5). In contrast, the sample containing a mixture of **M2** and **12** showed negligible change in the squaraine fluorescence wavelength over 120 h. Furthermore, there was very weak fluorescence energy transfer from excited **M2** to squaraine **12** (middle of Figure 5). Confirmation that **M2** remained empty was gained by conducting an experiment that added squaraine **13** to an equimolar solution of **M2** and **12**. As shown in the bottom of Figure 5, addition of **13** immediately formed **M2** ⊃

Scheme 4. Synthesis of 9 and Structure of 13

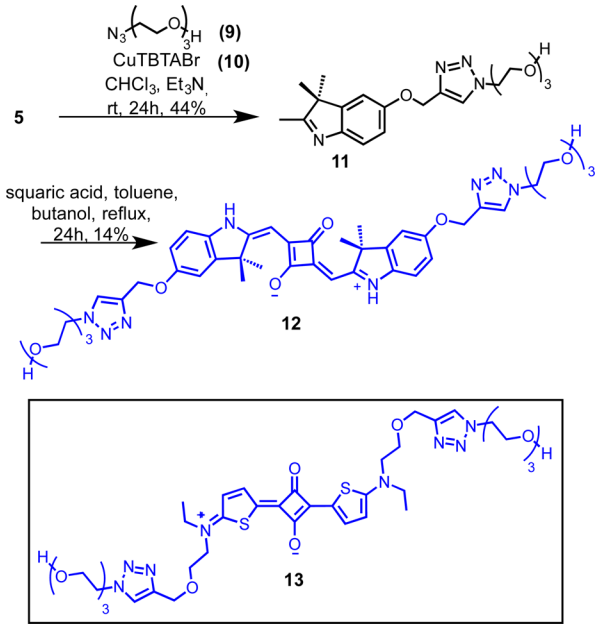

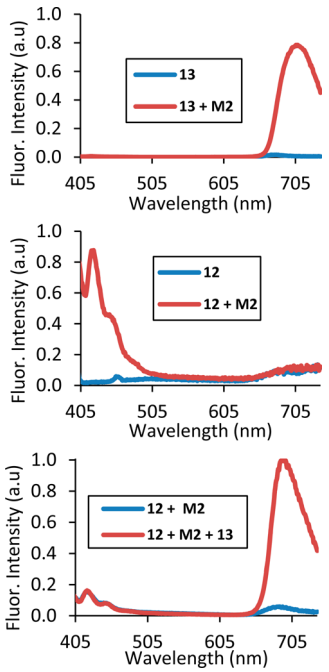

Figure 5. Fluorescence spectra showing efficiency of fluorescence energy transfer from excited **M2** (ex: 390 nm) to squaraine dye for different samples in water. (Top) Squaraine **13** and a mixture of **13** + **M2**, each component 3 μM. (Middle) Squaraine **12** and a mixture **12** + **M2**, each component 3 μM. (Bottom) Squaraine **13** and a mixture of **12** + **M2** + **13**, each component 3 μM.

13 as judged by the efficient energy transfer from excited **M2** and diagnostic red-shifted squaraine fluorescence. These results demonstrate that **M2** can be threaded by squaraine **13** but not by 3,3-dimethylindoline squaraine **12**. Thus, we conclude that the *gem*-dimethyl groups in 3,3-dimethylindoline squaraines are large enough to stop threading of anthracene-containing tetralactam **M1** or **M2** in chloroform and water, respectively. This is a notable finding since the combined steric bulk of the *gem*-dimethyl groups is quite small, but it is consistent with our

DOI: 10.1021/acs.joc.7b00655
J. Org. Chem. 2017, 82, 5819−5825

previous observations that squaraine substituents of comparative size and close proximity to the central C_4O_2 core can greatly hinder the kinetics of macrocycle threading.[24]

CONCLUSION

The *gem*-dimethyl groups in 3,3-dimethylindoline squaraine dyes are large enough to prevent threading or unthreading of rotaxanes when the surrounding macrocycle is a tetralactam with anthracene sidewalls. The organic soluble squaraine rotaxanes **M1** ⊃ **1** and **M1** ⊃ **2** were prepared by templated clipping reactions, and an X-ray structure of **M1** ⊃ **2** shows that the squaraine *gem*-dimethyl groups force a relatively wide separation between the two anthracene sidewalls in the surrounding macrocycle. The decreased interaction between the encapsulated squaraine and the anthracene sidewalls leads to a smaller red shift of the squaraine absorption and emission bands. Compound **M1** ⊃ **1** is the first example of an orange-emitting squaraine rotaxane and the large enhancement in squaraine fluorescence quantum yield upon encapsulation as a rotaxane nicely illustrates the enhancement in fluorescence performance that can be gained by dye encapsulation. The successful preparation of **M1** ⊃ **1** completes a palette of squaraine rotaxane fluorophores whose emission profiles span the color range from green to near-infrared.

EXPERIMENTAL SECTION

Synthesis. The synthesis and characterization of compounds **M1**,[6] **M2**,[25] **3**,[26] **8**,[6] **9**,[27] **10**,[28] and **13**[24] have been reported elsewhere and are not included here.

Hydrazine 4. Aniline derivative **3** (2.71 g, 18.4 mmol) was added to concentrated HCl (100 mL) and cooled to −5 °C in an ice−brine bath. $NaNO_2$ (1.77 g, 25.6 mmol) was dissolved in water (15 mL), and the solution was added dropwise into the reaction flask. The resulting solution was stirred at 0 °C for 2 h. $SnCl_2{\cdot}2H_2O$ (6.0 g, 31.6 mmol) was suspended in cold, concentrated HCl, and the resulting solution was slowly added to the reaction flask. The reaction was stirred at 0 °C for an additional 3 h. The precipitate was filtered, washed with brine (50 mL), collected, and suspended in NaOH solution. The product was extracted with CH_2Cl_2 (4 × 50 mL). The combined organic layers were dried over Na_2SO_4 and evaporated under reduced pressure to yield hydrazine **4** (1.53 g, 9.44 mmol, 51% yield) as a light yellow oil, which was used without further purification. ^{1}H NMR (500 MHz, $CDCl_3$) δ 6.88−6.92 (m, 2H), 6.75−6.79 (m, 2H), 4.62 (d, J = 2.4 Hz, 2H), 3.05−4.32 (br s, 3H), 2.52 (t, J = 2.4 Hz, 1H); ^{13}C NMR (125 MHz, $CDCl_3$) δ 151.4, 146.3, 116.3, 113.6, 79.2, 75.4, 56.7.

Indole 5. 3-Methyl-2-butanone (1.0 mL) and catalytic HCl were added to a solution of hydrazine **4** (1.09 g, 6.24 mmol) in ethanol (40 mL, 200 proof), and the reaction was refluxed in an oil bath for 20 h. The reaction was cooled to rt, and the ethanol was evaporated under reduced pressure. The resulting oil was suspended in water, and product was extracted with $CHCl_3$ (3 × 20 mL). The combined organic layers were dried over Na_2SO_4, evaporated under reduced pressure, and purified via column chromatography (10% EtOAc in $CHCl_3$) to yield indole **5** (437 mg, 2.05 mmol, 33% yield) as a light brown solid. ^{1}H NMR (500 MHz, $CDCl_3$) δ 7.34 (d, J = 8.4 Hz, 1H), 6.82 (d, J = 2.6 Hz, 1H), 6.78−6.81 (m, 1H), 4.59 (d, J = 2.4 Hz, 2H), 2.46 (t, J = 2.4 Hz, 1H), 2.14 (s, 3H), 1.17 (s, 6H); ^{13}C NMR (125 MHz, $CDCl_3$) δ 186.1, 155.6, 147.9, 147.1, 119.9, 113.0, 109.2, 78.6, 75.5, 56.1, 53.6, 23.0, 15.2. HRMS (ESI-TOF) m/z: $[M + H]^+$ calcd for $C_{14}H_{16}NO$ 214.1226; found 214.1235.

Semisquaraine 6. Indole **5** (437 mg) was dissolved in excess iodomethane (6.0 mL) and stirred for 6 h at rt. The indolium iodide salt (439 mg, 1.236 mmol) precipitated. ^{1}H NMR (500 MHz, DMSO-d_6) δ 7.84 (d, J = 8.8 Hz, 1H), 7.51 (d, J = 2.6 Hz, 1H), 7.20 (dd, J = 2.6 Hz, J = 8.8 Hz, 1H), 4.94 (d, J = 2.4 Hz, 2H), 3.94 (s, 3H), 3.63 (t, J = 2.4 Hz, 1H), 2.69−2.72 (m, 3H), 1.51 (s, 6H) and without further purification was suspended in ethanol (10 mL, 200 proof) under an atmosphere of argon. Triethylamine (0.20 mL) was added dropwise, immediately followed by the addition of diethyl squarate (232.1 mg, 1.364 mmol) in ethanol (5 mL). The reaction was stirred for 2 h at rt, at which time the solvent was evaporated under reduced pressure and semisquaraine **6** (287 mg, 0.817 mmol, 66% yield) was purified using column chromatography (10% EtOAc in $CHCl_3$) to yield a light brown solid. ^{1}H NMR (600 MHz, $CDCl_3$) δ 6.95 (d, J = 2.3 Hz, 1H), 6.90 (dd, J = 2.6 Hz, J = 8.5 Hz, 1H); 6.81 (d, J = 8.5 Hz, 1H), 5.30 (s, 1H), 4.89 (q, J = 7.1 Hz, 2H), 4.69 (d, J = 2.6 Hz, 2H), 3.35 (s, 3H), 2.54 (t, J = 2.3 Hz, 1H), 1.62 (s, 6H), 1.53 (t, J = 7.1 Hz, 3H); ^{13}C NMR (150 MHz, $CDCl_3$) δ 192.7, 187.5, 187.4, 173.7, 169.2, 154.4, 142.5, 137.8, 113.7, 110.8, 108.6, 81.4, 78.7, 75.9, 70.1, 56.8, 48.3, 30.3, 27.1, 16.1; HRMS (ESI-TOF) m/z: $[M + H]^+$ calcd for $C_{21}H_{22}NO_4$ 352.1543; found 352.1566.

Squaraine 7. Semisquaraine **6** was first hydrolyzed with NaOH using a previously published protocol.[26] The hydrolyzed product (74 mg, 0.230 mmol) was suspended in anhydrous *n*-butanol (25 mL) and benzene (25 mL) with aniline **3** (24 mg, 0.163 mmol). The reaction was refluxed in an oil bath for 10 h with azeotropic removal of water. Concentration under reduced pressure afforded crude product that was purified by column chromatography (20% to 40% acetone in $CHCl_3$) to yield **7** as an orange-red solid (74.9 mg, 0.166 mmol, 72% yield). ^{1}H NMR (500 MHz, $CDCl_3$) δ 7.76 (d, J = 8.2 Hz, 2H), 6.98−7.03 (m, 5H), 5.71 (s, 1H), 4.74 (d, J = 2.4 Hz, 2H), 4.71 (d, J = 2.4 Hz, 2H), 3.58 (s, 3H), 2.56 (t, J = 2.4 Hz, 1H), 2.55 (t, J = 2.4 Hz, 1H), 1.72 (s, 6H); ^{13}C NMR was not acquired due to very poor solubility of squaraine **S7**; HRMS (ESI-TOF) m/z: $[M + H]^+$ calcd for $C_{28}H_{25}N_2O_4$ 453.1809; found 453.1835.

Rotaxane M1 ⊃ 1. Squaraine **7** (1.1 mg, 2.2 μmol) and macrocycle **M1** (1.8 mg, 2.1 μmol) were combined in $CHCl_3$ to form pseudorotaxane **M1** ⊃ **7**. Azide **8** (4 mg, 8 μmol), DIPEA (2 drops), and organic soluble tris[(1-benzyl-1*H*-1,2,3-triazol-4-yl)-methyl]amine copper(I) bromide **10** (0.87 mg, 1.2 μmol) were added, and the reaction was stirred at rt for 12 h. The reaction was washed with an aqueous saturated EDTA solution, and the organic layer was isolated. Concentration under reduced pressure provided crude product that was further purified by column chromatography (20% EtOAc in $CHCl_3$) to yield **M1** ⊃ **1** (2.7 mg, 1.5 μmol, 71% yield) as a pink solid. Mp >260 °C; ^{1}H NMR (600 MHz, $CDCl_3$) δ 9.01 (s, 1H), 8.90 (s, 1H), 8.49 (s, 2H), 8.47 (s, 2H), 8.04 (t, J = 3.5 Hz, 2H), 7.97 (d, J = 8.8 Hz, 2H), 7.87−7.91 (m, 4H), 7.77 (d, J = 8.8 Hz, 2H), 7.70 (s, 1H), 7.47−7.52 (m, 6H), 7.40 (t, J = 7.4 Hz, 2H), 7.36 (d, J = 7.4 Hz, 4H), 7.23−7.27 (m, 6H), 7.18−7.22 (m, 9H), 7.16 (t, J = 7.0 Hz, 2H), 7.12 (d, J = 8.8 Hz, 2H), 6.89 (t, J = 7.6 Hz, 2H), 6.85 (d, J = 9.4 Hz, 1H), 6.74−6.78 (m, 6H), 6.67−6.70 (m, 2H), 6.53 (d, J = 7.6 Hz, 1H), 6.43 (d, J = 9.4 Hz, 1H), 6.32−6.37 (m, 3H), 5.75 (dd, J = 8.2 Hz, J = 14.7 Hz, 2H), 5.19 (s, 2H), 5.14−5.17 (m, 4H), 4.89 (d, J = 15.0 Hz, 2H), 4.87 (s, 4H), 4.54 (t, J = 7.0 Hz, 2H), 4.01 (t, J = 5.9 Hz, 2H), 3.89 (s, 1H), 2.20 (pent, J = 7.3 Hz, 2H), 1.86 (pent, J = 5.9 Hz, 2H), 1.52 (s, 9H), 1.51 (s, 9H); ^{13}C NMR (150 MHz, $CDCl_3$) δ 175.3, 173.3, 171.2, 168.0, 166.7, 166.4, 165.4, 156.6, 155.6, 147.0, 143.7, 143.6, 140.6, 139.3, 139.3, 137.1, 133.2, 133.0, 132.4, 132.4, 131.2, 130.6, 130.3, 130.2, 130.1, 129.8, 129.7, 129.2, 128.5, 128.0, 127.6, 126.0, 126.0, 125.8, 125.4, 123.9, 123.8, 123.5, 123.5, 123.4, 123.4, 123.4, 123.3, 123.2, 123.1, 123.1, 123.0, 122.0, 120.6, 120.5, 120.5, 120.5, 120.5, 120.5, 120.5, 114.9, 113.9, 113.2, 113.1, 110.4, 110.3, 66.8, 64.3, 62.6, 62.3, 50.4, 50.4, 49.9, 35.6, 31.6, 29.9, 27.9, 27.7, 27.6, 26.3; HRMS (ESI-TOF) m/z: $[M + H]^+$ calcd $C_{142}H_{131}N_{12}O_{10}$ 2164.0106; found 2164.0081.

Squaraine 1. Squaraine **7** (16 mg, 35 μmol), azide **8** (38 mg, 87 μmol), DIPEA (3 drops), and organic soluble tris[(1-benzyl-1*H*-1,2,3-triazol-4-yl)methyl]amine copper(I) bromide **10** (1.6 mg, 2.5 μmol) were dissolved in $CHCl_3$ (10 mL). The reaction was stirred at rt for 5 h. The solution was then washed with an aqueous saturated EDTA solution, and the organic layer was isolated. Concentration under reduced pressure afforded crude product that was further purified by column chromatography (30 to 50% acetone in $CHCl_3$) to yield **1** (29 mg, 22 μmol, 62% yield) as a red solid. ^{1}H NMR (600 MHz, $CDCl_3$) δ ^{1}H NMR (600 MHz, $CDCl_3$) δ 7.93 (d, J = 7.9 Hz, 2H), 7.69 (s, 1H), 7.66 (s, 1H), 7.22−7.26 (m, 12H), 7.17−7.21 (m, 18H), 7.10 (dd, J =

DOI: 10.1021/acs.joc.7b00655
J. Org. Chem. 2017, 82, 5819−5825

2.6 Hz, J = 9.1 Hz, 4H), 7.03 (s, 1H), 6.99 (d, J = 8.5 Hz, 2H), 6.95 (dd, J = 2.0 Hz, J = 8.2 Hz, 1H), 6.88 (d, J = 8.5 Hz, 1H), 6.74 (dd, J = 2.0 Hz, J = 8.8 Hz, 4H), 5.76 (s, 1H), 5.22 (s, 2H), 5.21 (s, 2H), 4.46 (t, J = 7.0 Hz, 2H), 4.45 (t, J = 7.0 Hz, 2H), 3.96 (t, J = 5.8 Hz, 4H), 3.46 (s, 3H), 2.13 (sex, J = 5.9 Hz, 4H), 1.78−1.83 (m, 6H), 1.72−1.78 (m, 4H); ^{13}C NMR (150 MHz, $CDCl_3$) δ 156.8, 156.8, 156.0, 147.2, 147.2, 139.4, 139.4, 132.4, 132.4, 131.3, 127.6, 127.6, 126.1, 126.0, 122.0, 115.7, 113.3, 110.7, 70.8, 66.9, 64.5, 63.0, 62.6, 54.0, 50.3, 29.9, 29.5, 27.5, 27.5, 26.4, 26.4; HRMS (ESI-TOF) m/z: $[M + H]^+$ calcd for $C_{86}H_{79}N_8O_6$ 1319.6117; found 1319.6133.

Squaraine ***2***. 5-Methoxy-2,3,3-trimethyl-3*H*-indole (478 mg, 2.52 mmol) and squaric acid (145 mg, 1.26 mmol) were dissolved in 20 mL of toluene and butanol and then refluxed in an oil bath for 24 h. The solvent was removed under reduced pressure to yield the crude material. The crude material was purified by column chromatography (0−10% acetone in dichloromethane) to yield the dark blue solid **2** (238 mg, 0.522 mmol, 41% yield). Mp 255−260 °C; ^{1}H NMR (400 MHz, $CDCl_3$) δ 12.7 (s, 1H), 12.4 (s, 1H), 7.02 (d, J = 8.3 Hz, 1H), 6.79 (m, 4H), 6.69 (d, J = 8.3 Hz, 1H), 5.37 (s, 1H), 5.30 (s, 1H), 3.74 (s, 6H), 1.36 (s, 12H); ^{13}C NMR (400 MHz, $CDCl_3$) δ 183.5, 175.1, 174.6, 174.2, 173.5, 156.6, 140.7, 135.7, 112.7, 110.8, 109.6, 85.3, 55.9, 48.9, 26.7; HRMS (ESI-TOF) m/z: $[M + H]^+$ calcd for $C_{28}H_{28}N_2O_4$ 457.2049; found 457.2063.

Rotaxane ***M1*** ⊃ ***2***. Squaraine **2** (166 mg, 0.703 mmol) was dissolved in 150 mL of anhydrous $CHCl_3$. 5-*tert*-Butylisophthaloyl dichloride (183 mg, 0.713 mmol) and a mixture of 9,10-bis(aminomethyl)anthracene (64 mg, 0.140 mmol) and *N*,*N*-diisopropylethylamine (160 μL, 1.15 mmol) were each dissolved in 80 mL of anhydrous $CHCl_3$. Each solution was drawn into separate syringes and added dropwise over a period of 8 h by a syringe pump to the squaraine **2** solution under argon gas. The solvent was removed under reduced pressure, and the crude product was isolated by column chromatography (0−10% acetone in chloroform) to yield **M1** ⊃ **2** (19.5 mg, 15 μmol, 11% yield) as a sea green solid. Mp >260 °C; ^{1}H NMR (600 MHz, $CDCl_3$) δ 10.1 (d, 2H), 8.58 (d, 4H) 8.44 (t, 2H), 8.07 (d, J = 6.0 Hz, 4H), 7.89 (d, J = 6.0 Hz, 4H), 7.50 (d, J = 6.0 Hz, 4H), 6.92 (m, 4H) 6.85 (m, 4H), 6.83 (m, 4H), 6.70 (s, 2H), 5.67 (dd, J = 6 Hz, J = 12 Hz 4H), 5.21 (dd, J = 12 Hz, 4H), 3.97 (s, 2H), 3.88 (s, 6H), 1.54 (s, 18H), 0.91 (s, 12H); ^{13}C NMR (400 MHz, $CDCl_3$) δ 181.4, 173.4, 167.2, 166.4, 165.8, 157.0, 153.2, 148.1, 147.6, 140.3, 133.2, 130.0, 129.8, 129.0, 126.3, 125.9, 124.7, 124.0, 120.3, 112.7, 112.5, 109.0, 83.2, 55.9, 48.5, 37.2, 35.4, 31.4, 29.7, 27.8; HRMS (ESI-TOF) m/z: $[M + Na]^+$ calcd for $C_{84}H_{80}N_6O_8Na$ 1323.5930; found 1323.5932.

Indole ***11***. Indole **5** (0.2261 g, 1.06 mmol), **9** (0.5682 g, 3.35 mmol), triethylamine (0.9 mL, 6.36 mmol), and copper(I) tris[(1-benzyl-1*H*-1,2,3-triazol-4-yl)methyl]amine bromide **10** (0.265 mmol, 0.25 molar equivalence) were dissolved in 5 mL of chloroform and stirred at room temperature overnight. The reaction mixture was filtered through Celite and then purified by column chromatography (0−50% methanol in chloroform) to yield a brown yellow oil containing **11** (180 mg, 0.464 mmol, 44% yield) ∼80% purity with ∼20% unreacted **9**. This material was carried to the next step. ^{1}H NMR (500 MHz, $CDCl_3$) δ 7.76 (s, 1H), 7.35 (d, J = 8.3 Hz, 1H), 6.87 (d, J = 2.2 Hz, 1H), 6.84 (dd, J = 2.4 Hz, J = 8.3 Hz, 1H), 5.16 (s, 2H), 4.49 (t, J = 10 Hz, 2H), 3.83 (t, J = 10 Hz, 2H), 3.53 (s, 4H), 3.49 (t, J = 10 Hz, 2H), 3.32 (t, J = 10 Hz, 2H), 2.17 (s, 3H), 1.21 (2, 6H); ^{13}C NMR (400 MHz, $CDCl_3$) δ 186.3, 147.8, 129.1, 124.0, 120.1, 113.2, 109.2, 72.5, 72.5, 71.4, 70.7, 70.6, 70.4, 70.3, 70.1, 69.4, 62.6, 61,8, 61.8, 50.7, 50.3, 23.2, 15.3; HRMS (ESI-TOF) m/z: $[M + H]^+$ calcd for $C_{20}H_{29}N_4O_4$ 389.21833; found 389.2210.

Squaraine ***12***. Indole **11** (0.1818 g, 0.468 mmol) and squaric acid (0.0277g, 0.243 mmol) were dissolved in 10 mL of toluene and butanol and then refluxed in an oil bath overnight. The solvent was removed under reduced pressure, and the crude product was subjected to column chromatography (0−30% methanol in chloroform) to yield a green film. The film was dissolved in $CHCl_3$ and washed repeatedly with deionized water until the aqueous layer was no longer yellow. The solvent was removed under pressure to yield the dark green film **12** (30 mg, 35 μmol, 14% yield). ^{1}H NMR (600 MHz, $CDCl_3$) δ 12.7 (s, 1H), 12.4 (s, 1H), 7.83 (s, 2H), 7.08 (d, J = 8.3 Hz, 1H), 7.02 (d, J = 8.3 Hz, 1H), 6.90 (m, 4H), 5.36 (s, 1H), 5.18 (s, 4H), 4.55 (m, 4H), 3.88 (m, 4H), 3.71 (m, 4H), 3.59 (m, 8H), 3.55 (m, 4H), 1.41 (s, 12H). ^{13}C NMR (500 MHz, $CDCl_3$) δ 155.1, 143.2, 140.4, 124.2, 113.7, 111.4, 110.2, 84.6, 72.1, 70.0, 69.7, 68.8, 61.9, 60.7, 48.6, 48.4, 48.1, 47.9, 47.7, 47.5, 25.8; HRMS (ESI-TOF) m/z: $[M + H]^+$ calcd for $C_{44}H_{54}N_8O_{10}$ 855.3963; found 855.4046.

X-ray Structure of Rotaxane ***M1*** ⊃ ***2***. An arbitrary sphere of data was collected on a green plate-like crystal, having approximate dimensions of 0.207 × 0.123 × 0.023 mm^3, on a Bruker APEX-II diffractometer using a combination of ω- and φ-scans of 0.5°. Data were corrected for absorption and polarization effects and analyzed for space group determination. The structure was solved by intrinsic phasing methods and expanded routinely.[29] The model was refined by full-matrix least-squares analysis of F^2 against all reflections.[30] All non-hydrogen atoms were refined with anisotropic atomic displacement parameters. Unless otherwise noted, hydrogen atoms were included in calculated positions. Atomic displacement parameters for the hydrogens were tied to the equivalent isotropic displacement parameter of the atom to which they are bonded (U_{iso}(H) = 1.5U_{eq}(C) for methyl, 1.2U_{eq}(C) for all others). Diffraction analysis shows two molecules of the ring/thread pair in the unit cell of the primitive, centrosymmetric, monoclinic space group $P2_1/c$. The ring/thread molecule pair crystallizes about a center of symmetry [0.5, 0.5, 0.5]; thus, only half of each of the two molecules is required to describe the full molecular species present in the solid state. There is rotational disorder present in the *t*-Bu group of the rotaxane and it was modeled over three positions, with occupancies refined for each and summed to unity, yielding an approximately 0.5:0.3:0.2 site occupancy ratio. The carbon atoms were modeled with isotropic atomic displacement parameters; all other non-hydrogen atoms were refined as an anisotropic model. The amide/amine hydrogen atoms (N1, N2, N3) were all located from a difference Fourier map and subsequently refined as a riding model.

Crystal data for $C_{84}H_{80}N_6O_8$; M_r = 1301.54; Monoclinic; space group $P2_1/c$; a = 10.9997(5) Å; b = 25.0507(12) Å; c = 13.0048(6) Å; α = 90°; β = 112.420(3)°; γ = 90°; V = 3312.6(3) Å^3; Z = 2; T = 120(2) K; λ(Cu Kα) = 1.54184 Å; μ(Cu Kα) = 0.669 mm^{-1}; d_{calc} = 1.305 g·cm^{-3}; 44 055 reflections collected; 6502 unique (R_{int} = 0.0522); giving R_1 = 0.0779, wR_2 = 0.2227 for 5314 data with [$I > 2\sigma(I)$] and R_1 = 0.0896, wR_2 = 0.2358 for all 6502 data. Residual electron density (e$^-$·Å^{-3}) max/min: 0.921/−0.310.

■ ASSOCIATED CONTENT

Supporting Information

The Supporting Information is available free of charge on the ACS Publications website at DOI: 10.1021/acs.joc.7b00655.

Copies of spectra for all new compounds (PDF)

X-ray crystallography information (CIF)

■ AUTHOR INFORMATION

Corresponding Author

*E-mail: smith.115@nd.edu.

ORCID

Bradley D. Smith: 0000-0003-4120-3210

Notes

The authors declare no competing financial interest.

■ ACKNOWLEDGMENTS

This work was supported by the NSF (CHE1401783) and the University of Notre Dame. We thank Wenqi Liu for valuable assistance with molecular modeling.

■ REFERENCES

(1) Dsouza, R. N.; Pischel, U.; Nau, W. M. *Chem. Rev.* **2011**, *111*, 7941−7980.

(2) Dsouza, R. N.; Hennig, A.; Nau, W. M. *Chem. - Eur. J.* **2012**, *18*, 3444−3459.
(3) Gassensmith, J. J.; Baumes, J. M.; Smith, B. D. *Chem. Commun.* **2009**, 6329−6338.
(4) Arunkumar, E.; Forbes, C. C.; Noll, B. C.; Smith, B. D. *J. Am. Chem. Soc.* **2005**, *127*, 3288−3289.
(5) Johnson, J. R.; Fu, N.; Arunkumar, E.; Leevy, W. M.; Gammon, S. T.; Piwnica-Worms, D.; Smith, B. D. *Angew. Chem., Int. Ed.* **2007**, *46*, 5528−5531.
(6) Collins, C. G.; Peck, E. M.; Kramer, P. J.; Smith, B. D. *Chem. Sci.* **2013**, *4*, 2557−2563.
(7) Baumes, J. M.; Gassensmith, J. J.; Giblin, J.; Lee, J.-J.; White, A. G.; Culligan, W. J.; Leevy, W. M.; Kuno, M.; Smith, B. D. *Nat. Chem.* **2010**, *2*, 1025−1030.
(8) Collins, C. G.; Baumes, J. M.; Smith, B. D. *Chem. Commun.* **2011**, *47*, 12352−12354.
(9) Law, K. Y. *J. Phys. Chem.* **1995**, *99*, 9818−9824.
(10) Fu, C.; Lei, L.; Sun, K.; Xia, P.; Yuan, H.; Xiao, D.; Li, Z. *Renewable Energy* **2012**, *38*, 163−168.
(11) Patsenker, L. D.; Tatarets, A. L.; Klochko, O. P.; Terpetschnig, E. A. *Springer Ser. Fluoresc.* **2010**, *9*, 159−190.
(12) Fu, N.; Gassensmith, J. J.; Smith, B. D. *Supramol. Chem.* **2009**, *21*, 118−124.
(13) Encapsulation of 3,3-dimethylindoline squaraine **1** or **2** inside **M1** leads to a moderate red shift of 10−15 nm in the absorption and emission bands, which is about half the red shift observed when a bis(4-aminophenyl)squaraine is encapsulated inside **M1**. In the case of bis(4-aminophenyl)squaraine rotaxanes, the encapsulation process is thought to inhibit geometric deformations of the encapsulated squaraine and stabilize the squaraine excited state by electronic reorganization of the surrounding macrocycle; see: Jacquemin, D.; Perpete, E. A.; Laurent, D.; Assfeld, X.; Adamo, C. *Phys. Chem. Chem. Phys.* **2009**, *11*, 1258−1262. The smaller red shifts with 3,3-dimethylindoline squaraine rotaxanes is likely due to the wider centroid-to-centroid distance between the two anthracene sidewalls in the surrounding macrocycle which is necessary to accommodate the squaraine gem-dimethyl groups. This means weaker interactions between the anthracene sidewalls and the encapsulated squaraine excited state.
(14) Martinez-Cuezva, A.; Rodrigues, L. V.; Navarro, C.; Carro-Guillen, F.; Buriol, L.; Frizzo, C. P.; Martins, M. A. P.; Alajarin, M.; Berna, J. *J. Org. Chem.* **2015**, *80*, 10049−10059.
(15) Felder, T.; Schalley, C. A. *Angew. Chem., Int. Ed.* **2003**, *42*, 2258−2260.
(16) Tachibana, Y.; Kihara, N.; Furusho, Y.; Takata, T. *Org. Lett.* **2004**, *6*, 4507−4509.
(17) Saito, S.; Takahashi, E.; Wakatsuki, K.; Inoue, K.; Orikasa, T.; Sakai, S.; Yamasaki, R.; Mutoh, Y.; Kasama, T. *J. Org. Chem.* **2013**, *78*, 3553−3560.
(18) Han, X.; Liu, G.; Liu, S. H.; Yin, J. *Org. Biomol. Chem.* **2016**, *14*, 10331−10351.
(19) The large enhancement in fluorescence quantum yield for **1** when it is encapsulated to form **M1** ⊃ **1** is tentatively attributed to inhibited rotation of the N-aryl ring in **1** that occurs upon encapsulation (see the model in Figure 2). In the case of squaraine **2** there is no equivalent single bonded ring that can act as a rotor to mediate nonradiative energy decay. Thus, there is no increase in fluorescence quantum yield for **2** when it is encapsulated to form **M1** ⊃ **2**.
(20) Baumes, J. M.; Murgu, I.; Oliver, A.; Smith, B. D. *Org. Lett.* **2010**, *12*, 4980−4983.
(21) Dirk, C. W.; Herndon, W. C.; Henry, F. C.; Martinez, S.; Kalamegham, P.; Tan, A.; Campos, G.; Velez, M.; Zyss, J.; Ledoux, I.; Chengg, L. *J. Am. Chem. Soc.* **1995**, *117*, 2214−2225.
(22) Li, Z.; Xu, S.; Huang, L.; Huang, X.; Niu, L.; Chen, Z.; Zhang, Z.; Zhang, F.; Kasatani, K. *Chem. Phys. Lett.* **2007**, *441*, 123−126.
(23) Peck, E. M.; Liu, W.; Spence, G. T.; Shaw, S. K.; Davis, A. P.; Destecroix, H.; Smith, B. D. *J. Am. Chem. Soc.* **2015**, *137*, 8668−8671.
(24) Liu, W.; Peck, E. M.; Hendzel, K. D.; Smith, B. D. *Org. Lett.* **2015**, *17*, 5268−5271.
(25) Ke, C.; Destecroix, H.; Crump, M. P.; Davis, A. P. *Nat. Chem.* **2012**, *4*, 718−723.
(26) Gacal, B. N.; Filiz, V.; Abetz, V. *Macromol. Chem. Phys.* **2016**, *217*, 672−682.
(27) Brun, M. A.; Tan, K. T.; Griss, R.; Kielkowska, A.; Reymond, L.; Johnsson, K. *J. Am. Chem. Soc.* **2012**, *134*, 7676−7678.
(28) Donnelly, P. S.; Zanatta, S. D.; Zammit, S. C.; White, J. M.; Williams, S. J. *Chem. Commun.* **2008**, *41*, 2459−2461.
(29) Sheldrick, G. M. *Acta Crystallogr., Sect. A: Found. Adv.* **2015**, *71*, 3−8.
(30) Sheldrick, G. M. *Acta Crystallogr., Sect. C: Struct. Chem.* **2015**, *71*, 3−8.

DOI: 10.1021/acs.joc.7b00655
J. Org. Chem. 2017, 82, 5819−5825